Wiley Online Library
Early View publication on www.wileyonlinelibrary.com
(issue and page numbers not yet assigned;
citable using Digital Object Identifier – **DOI**)

Phys. Status Solidi A, 1700321 (2017) / **DOI** 10.1002/pssa.201700321

physica status solidi a
www.pss-a.com
applications and materials science

Light-induced degradation in quasi-monocrystalline silicon PERC solar cells: Indications on involvement of copper

Henri Vahlman*[,1], Matthias Wagner[2], Franziska Wolny[2], Andreas Krause[2], Hannu Laine[1], Alessandro Inglese[1], Marko Yli-Koski[1], and Hele Savin[1]

[1] Department of Electronics and Nanoengineering, Aalto University, Tietotie 3, 02150 Espoo, Finland
[2] SolarWorld Innovations GmbH, Berthelsdorfer Str. 111A, 09599 Freiberg, Germany

Received 9 March 2017, revised 23 May 2017, accepted 24 May 2017
Published online 12 June 2017

Keywords copper, gettering, impurities, light-induced degradation, silicon, solar cells

* Corresponding author: e-mail henri.vahlman@aalto.fi, Phone: +358 50 431 8869

High-efficiency solar cell designs such as the passivated emitter and rear cell (PERC) raise the quality requirements for silicon substrates, favoring monocrystalline materials. Seed-cast quasi-monocrystalline silicon (qm-Si) is a promising alternative for Czochralski (Cz) Si with potential benefits of lower cost and reduced energy footprint. However, the purity and crystalline quality of qm-Si is not on par with Cz-Si, which can cause efficiency losses for example in the form of light-induced degradation (LID). In this contribution, we study the LID phenomena that can be present in qm-Si PERC solar cells, and compare them to the Cz-Si PERC. Degradation and regeneration are analyzed especially from the viewpoint of Cu impurity, which has until very recently been omitted as a source of LID for this device type. Subsequently, differences in LID behavior between qm-Si and Cz-Si are investigated considering the density of dislocations in the bulk. The results imply that slurry-based wafer slicing may introduce contamination that is capable of causing considerable LID in PERC devices fabricated of Si with inherently high defect density.

1 Introduction Passivated emitter and rear contact (PERC) solar cell is on its way to becoming a major commercial architecture [1]. Due to an effective surface passivation, PERC cells have a higher efficiency potential than the standard aluminum back-surface field (Al-BSF) cells. Harnessing the full benefits of this cell structure requires a high bulk minority carrier lifetime of several hundred μs [2, 3], which makes the PERC architecture more susceptible to metallic impurities and raises the standards for the silicon starting material in terms of material purity.

While Czochralski silicon (Cz-Si) provides high lifetimes and is therefore the natural choice for PERC cells, the Cz process is slower and more energy-intensive than casting of multi-crystalline Si (mc-Si) [4]. This results in potentially shorter energy payback times and lower cost per watt with cast Si. Yet, the bulk lifetime and consequently the PERC efficiency can be considerably limited in the case of mc-Si by metallic impurities [2, 5], grain boundaries, and extended defects originating from ingot growth [6, 7], which together with incompatibility with alkaline texturing present significant drawbacks [8]. A promising solution for these issues is to use seed crystals at the bottom of the casting crucible, resulting in largely monocrystalline material known as quasi-monocrystalline silicon (qm-Si), also referred to as cast-mono Si [9]. Although dislocation density in qm-Si can be high compared to Cz-Si [10, 11], lifetimes even in excess of 1 ms have been achieved [12].

As increasing bulk lifetimes are obtained, light-induced degradation (LID) effects gain in significance. Since Cz-Si contains a high concentration of interstitial O (O_i), this material is associated with considerable LID due to the BO defect (BO-LID) [13]. In cast-Si, BO-LID is mitigated by its lower [O_i], amounting to only 20% of [O_i] in Cz-Si [14]. However, several authors have recently reported

considerable, up to 10%$_{rel}$ light- and elevated temperature-induced degradation (LeTID [15]) both in mc-Si [15–22] and qm-Si [16] solar cells. In addition, so-called Sponge-LID was recently reported [23]. Furthermore, Cu impurity has been found to cause LID (Cu-LID) in p-type Si wafers [24–28] and solar cells [29]. Recently, Cu precipitates were observed in mc-Si PERCs with strong LID of 15%$_{rel}$ [30].

In this contribution, we evaluate the significance of the above-mentioned LID mechanisms in qm-Si PERC solar cells and lifetime samples with a particular focus on the effects of Cu, which are to date remain largely unreported. Open questions include: In industrial manufacturing conditions, is the gettering effect of a P-diffusion emitter sufficient for Cu mitigation? Are the effects of Cu stronger in some Si material types than others? To study these questions, degradation and regeneration behavior of qm-Si PERCs are analyzed and compared to results reported in the literature. We assess whether Cu can be present in the bulk after emitter formation and, in this context, we demonstrate the usefulness of the recently introduced surface charging method in distinguishing Cu-LID from other LID mechanisms [31]. Finally, we perform intentional Cu contamination experiments on lifetime samples to compare the effects of impurity Cu in qm-Si and Cz-Si bulk, and investigate the role of dislocations in Cu-LID.

2 Experimental Experimental process flow of this work is shown in Fig. 1. 180 μm thick 156 × 156 mm^2 wafers were sliced with a slurry-based multi-wire saw, followed by alkaline saw damage removal (SDR) and surface cleaning (HF/O_3). [O_i] was measured with Fourier transform infrared spectroscopy (FTIR). Surface [Cu] was determined with the total-reflection X-ray fluorescence (TXRF) method.

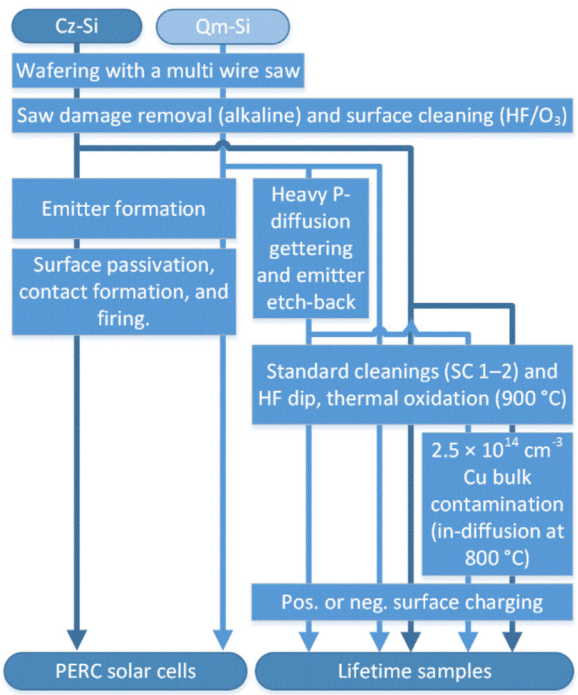

Figure 1 Experimental process flow of this work.

PERC cells were fabricated using Cz-Si (1.6 Ωcm) and qm-Si (1.2–2.0 Ωcm) in a standard industrial sequence. Lifetime samples were prepared both from Cz-Si (2.0 Ωcm) and mid-ingot qm-Si (1.2–2.0 Ωcm). For part of the qm-Si lifetime samples, heavy P-diffusion gettering emitter (40 Ω/□) was created with the $POCl_3$ process, followed by 2 h annealing at 680 °C, and double-sided emitter etch-back. All lifetime samples were standard-cleaned and surface passivated by thermal oxide formation at 900 °C for 40 min in O_2 and 20 min in N_2 atmosphere. Part of the lifetime samples were Cu contaminated by spin-coating a 1 ppm (w/v) Cu solution, followed by in-diffusion at 800 °C for 20 min in N_2, resulting in an interstitial Cu concentration of $[Cu_i] = 2.5 \times 10^{14}$ cm^{-3} [26]. A corona charge of either +0.4 or −0.8 μC cm^{-2} was deposited on top of the samples. Dislocation density was measured from sister wafers to the spin-contaminated qm-Si wafers via a Wright–Jenkins etch followed by etch-pit density (EPD) counting [32].

The PERC devices were illuminated under 0.5 sun at ∼50 °C. Regeneration was performed on a hotplate under 0.6 sun. *I*–*V* measurements were performed at standard testing conditions (STC) under 1 sun at 25 °C. The lifetime samples were aged under 0.65 sun either at 25 or 50 °C. Recovery anneal was performed by heating the lifetime sample for 10 min at 200 °C on a hotplate in the dark. The minority carrier lifetime was measured with Sinton quasi steady state photoconductance (QSSPC) instrument at an excess carrier concentration of 0.1 times the doping level. Lifetime maps were measured with Semilab microwave photoconductance decay (μPCD) instrument, and photoluminescence (PL) maps with BT imaging LIS R1 tool.

3 Results and discussion

3.1 LID in PERC solar cells Relative efficiencies of identically fabricated qm-Si and Cz-Si PERC solar cells under illumination are shown on the left half of Fig. 2. Both cell types had an initial efficiency of ∼19.5%. However, whereas the qm-PERCs exhibit a very strong LID between 12 and 16%$_{rel}$, the efficiency drop is only moderate (∼2%$_{rel}$) in the Cz-PERC. As mentioned above, BO-LID is expected to be markedly lower in qm-Si than in similarly doped Cz-Si due to much lower [O_i] (1–2 × 10^{17} vs. ∼5–8 × 10^{17} cm^{-3}). Thus, the BO defect is ruled out as the root cause for the strong LID present in qm-Si. On the other hand, the ∼2%$_{rel}$ LID seen in the Cz-PERC is in agreement with both experimental and simulated BO-LID in similar materials [33].

To investigate if LID observed in qm-Si shows similarity to LeTID or Sponge-LID, Fig. 3 shows a comparison between one of the qm-PERCs of Fig. 2 and literature data. Relative degradation in terms of both open circuit voltage, V_{oc}, and efficiency, η, is shown. The two

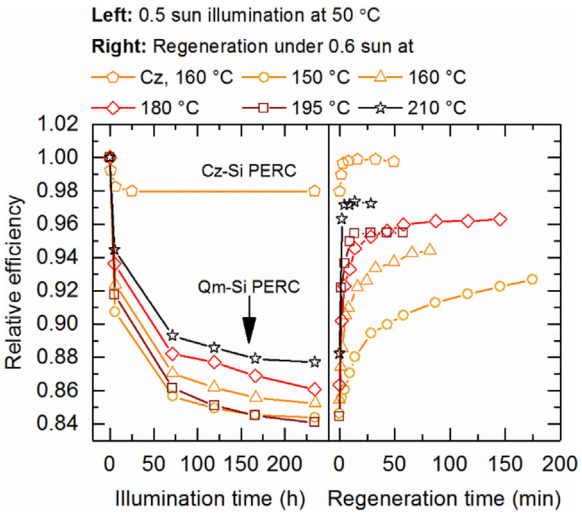

Figure 2 Degradation in the studied PERC solar cells under 0.5 sun illumination at 50 °C (left half), and subsequent regeneration (right half) at different temperatures.

groups can be distinguished based on the timescale of LID. (i): Very slow degradation on a timescale of tens or hundreds of hours associated with LeTID was reported in Refs. [15] and [16] in similar conditions as in this work. (ii): Faster LID in the cases of the qm-PERC of this work and Sponge-LID [23], in both of which at least 50% of the degradation occurs in less than ten hours of illumination.

Subsequent to LID, regeneration was observed at elevated temperatures (>150 °C) in both qm- and Cz-PERCs as shown on the right half of Fig. 2. The Cz-PERC exhibited full regeneration after only few minutes, which supports the above conclusion on BO-LID [34, 35]. On the other hand, all qm-PERCs regenerated only partially, and the final efficiency varied between ~3–7%$_{rel}$ below the initial level. We note here that regeneration in the qm-PERCs shows similarity to LeTID in its temperature-dependent behavior. Payne et al. [36] have reported that regeneration timescale of LeTID can be accelerated from between tens to hundreds of minutes to less than ten by increasing the temperature from 140 to 250 °C. This is comparable to the increase in the rate of regeneration in the qm-Si PERC cells when temperature is increased from 150 to 210 °C. After regeneration, the cells were re-illuminated under similar conditions (data not shown) with only a slight degradation.

Although the regeneration behavior of the qm-PERC shows similarity to earlier observations of LeTID, the degradation timescale in Fig. 3 differs notably. For example, 50% of LID occurs in ~5 h in the qm-PERC, whereas in case of LeTID the same takes tens or hundreds of hours under the same conditions. In addition, PL maps of the qm-PERCs after LID (not shown) showed laterally uneven degradation patterns that were especially heavy on defected areas such as on sub-grain boundaries. This behavior resembles that earlier reported for Sponge-LID [23], and differs from LeTID that is laterally uniform [37], or even slightly reduced, on top of grain boundaries as compared to intra-grain areas [22]. Hence, we conclude that previous observations of LeTID do not fully explain LID in the qm-PERC, but also other mechanisms should be considered as the root cause. Since the BO defect was excluded above, alternative mechanisms include Sponge-LID and Cu-LID (which may also be the same). The recent observation of Cu precipitates at grain boundaries and rear surface of mc-Si PERCs suggests that Cu may also be present in the bulk in an η-limiting role [30]. As lifetime spectroscopy results of Cu-LID [28] and LeTID [19, 21] indicate that they are two separate defect mechanisms, we continue dissecting the root cause in the following section using lifetime samples.

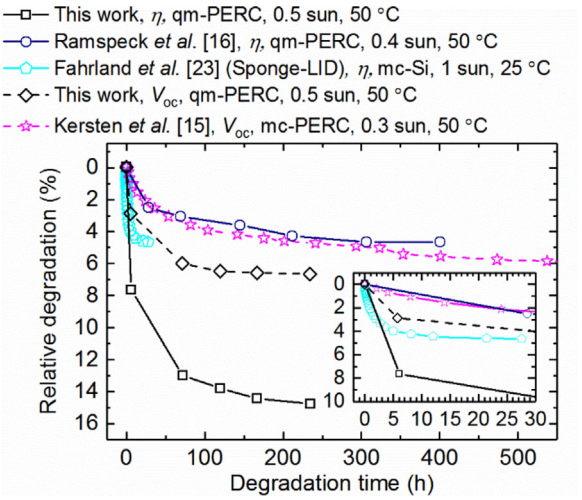

Figure 3 LID in the qm-PERC as compared to literature data [15, 16, 23] on LeTID and Sponge-LID. Relative degradation of either efficiency (η) or open circuit voltage (V_{oc}) is shown. All cells were degraded at open circuit. The inset is a zoom to the first 30 h.

3.2 Analysis of lifetime samples To investigate the role of Cu, qm-Si and Cz-Si lifetime samples are analyzed in this section. Figure 4 shows μPCD line scans

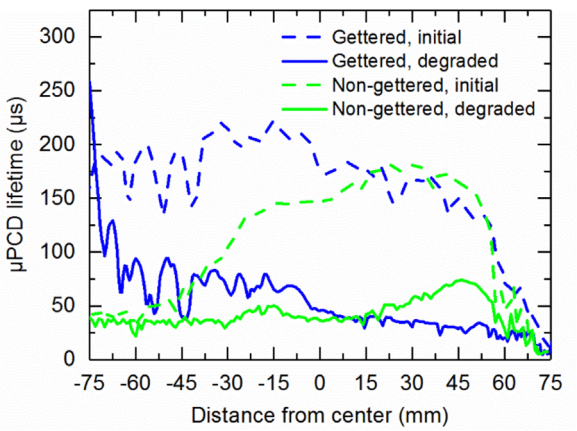

Figure 4 Line scans (30 mm wide) of μPCD maps of qm-Si lifetime samples both before and after LID.

over both a non-gettered and a gettered qm-Si sample. In the non-gettered wafer, large areas were strongly degraded already initially, whereas in the gettered sample these areas of poor initial lifetime were smaller suggesting efficient gettering of lifetime-limiting defects. However, considerable LID is observed in both cases upon illumination. Degradation patterns in the μPCD maps were of the same type as in the PL maps of qm-PERCs with pronounced LID on sub-grains.

The magnitude of LID in the qm-Si samples in comparison to Cz-Si is illustrated with QSSPC lifetimes in Fig. 5. The qm-Si samples showed much stronger degradation than the Cz-Si samples in which LID was in quantitative agreement with the BO defect [13, 14]. This is analogous with the behavior observed in the PERC solar cells in Fig. 2.

The above-discussed lifetime samples were surface passivated using a positive corona charge. Next, part of the qm-Si lifetime samples were deposited with a negative corona charge, which has previously been shown to prevent Cu-LID by attracting interstitial Cu from the bulk to the wafer surface [31]. Figure 5 shows that no LID was observed in the gettered qm-Si sample with a negative surface charge.

Cu-LID is the only LID mechanism reported to show dependence on surface charge [31, 38]. This clearly indicates that the final lifetime in the positively charged qm-Si samples is limited by Cu-LID. From that viewpoint, the partial recovery observed in gettered qm-Si in Fig. 5 is surprisingly high, since only very limited Cu-LID-related lifetime recovery has been reported [39]. However, as the magnitude of Cu-LID recovery has been shown to increase with decreasing [Cu] [39], the recovery in the gettered qm-Si may be explained by a lower [Cu] than in earlier studies. On the other hand, no recovery was observed in the non-gettered qm-Si sample. These results indicate that despite the partial removal of Cu during surface cleaning and heavy P-diffusion gettering, a notable [Cu] can remain in the bulk even after these process steps, thus causing a significant LID.

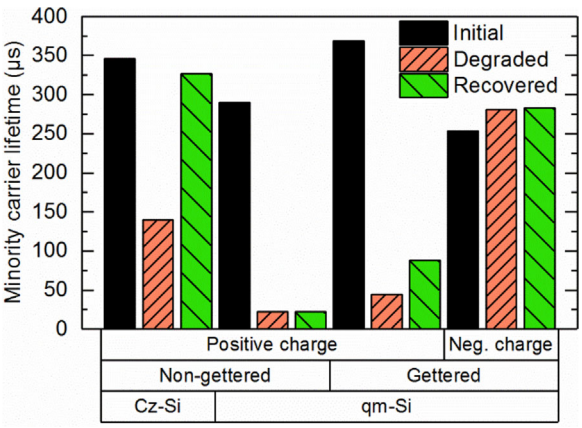

Figure 5 Initial, final, and recovered QSSPC lifetime on a central area of lifetime samples illuminated at 25 °C.

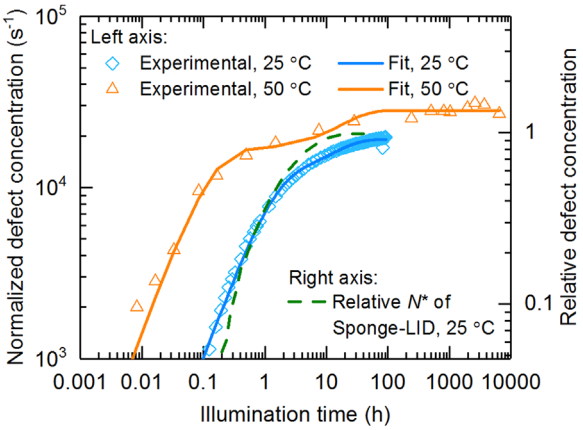

Figure 6 Left axis: Normalized defect concentration, N^*, of qm-Si lifetime samples illuminated at 25 and 50 °C at 0.65 sun. N^* was calculated based on experimental QSSPC lifetime and was fitted with Eq. (1). Right axis: Relative N^* of Sponge-LID based on solar cell data from Ref. [23] at 25 °C and 1 sun.

As Cu-LID is clearly the limiting mechanism in the qm-Si lifetime samples, and degradation patterns appear similar to those in solar cells, it is relevant to compare the timescale of LID observed in the lifetime samples with solar cells of Fig. 3. Figure 6 shows experimentally normalized defect concentration, N^*, in the gettered qm-Si lifetime samples at two different temperatures of 25 and 50 °C, in comparison to N^* of Sponge-LID [23]. N^* in lifetime samples was calculated as described in [13] and [27] based on the QSSPC lifetime. Due to a poor fit obtained by fitting experimental N^* with a single exponential rise, fitting was done using a double exponential rise as suggested for Cu-LID in Ref. [27]:

$$N^*_{\mathrm{fit}}(t) = N_{\mathrm{max},1}\left(1-\exp\left(-t/\tau_{\mathrm{fit},1}\right)\right) + N_{\mathrm{max},2}\left(1-\exp\left(-t/\tau_{\mathrm{fit},2}\right)\right), \quad (1)$$

where $N_{\mathrm{max},1}$, $N_{\mathrm{max},2}$, $\tau_{\mathrm{fit},1}$, and $\tau_{\mathrm{fit},2}$ are fitted with the least-squares method. This results in degradation time constants of $\tau_{\mathrm{fit},1} = 1.1$ h and $\tau_{\mathrm{fit},2} = 14$ h at 25 °C, and $\tau_{\mathrm{fit},1} = 0.11$ h and $\tau_{\mathrm{fit},2} = 21$ h at 50 °C. The lower $\tau_{\mathrm{fit},2}$ at 25 °C compared to the 50 °C data may be due to insufficient data at long illumination times in the first case, very slow asymptotic degradation [27], continuing even after the final lifetime measurement. At 50 °C, degradation continues slowly even after several hundreds or even thousands of hours, and therefore, the fitted time constants should be considered indicative at best. Nevertheless, the timescale of Cu-LID in the lifetime samples at 25 °C shows considerable resemblance to the timescale of Sponge-LID, and consequently to the initial part of LID in the qm-PERC in Fig. 3.

Regarding the origin of bulk Cu contamination in the lifetime sample wafers, a Cu concentration of $0.5–2 \times 10^{14}\,\mathrm{cm}^{-2}$ was measured on the surface of both

material types (Cz-Si and qm-Si) after slurry-based wafering and SDR, which is a typical value after these process steps [40]. Cu on the surface is expected to in-diffuse during following high-temperature steps, but even room temperature in-diffusion has been reported [41]. Due to uneven degradation patterns observed by μPCD imaging (see Fig. 4) that are untypical to bulk contamination from the ingot growth stage, we conclude that the root cause of LID in the qm-Si lifetime samples is most likely Cu contamination from the brass wires of the dicing saw. However, the fact that no correlation between the Si material type and surface Cu concentration was observed raises a question of why are the negative effects of Cu from this contamination source so much more pronounced in qm-Si than in Cz-Si. In the following section, this question is addressed based on the inherently higher density of dislocations in the qm-Si than in the Cz-Si bulk.

3.3 Dislocations and Cu-LID The role of dislocations in Cu-LID is examined by correlating the recombination activity of intentionally Cu contaminated mid-ingot qm-Si lifetime samples with dislocation density. A high bulk [Cu] of $2.5 \times 10^{14}\,cm^{-3}$ was used to reduce the significance of any preexisting LID compared to that caused by the intentional Cu contamination. Consequently, QSSPC lifetimes of the degraded qm-Si and Cz-Si wafers were ~5 μs and ~60 μs, respectively, which are sufficiently below those of Fig. 5 to cover the preexisting LID. Subsequently, the spatial coordinates of μPCD-maps taken before and after LID at 25 °C were matched, and the normalized defect density, N^*, was calculated for each pixel. After this, N^* of the Cu contaminated qm-Si wafers and EPD maps of sister wafers were similarly matched. This pixel-by-pixel comparison is plotted in Fig. 7. EPD of Cz-Si being below the detection limit ($10^{-2}\,cm^{-2}$), a comparison to qm-Si in Fig. 7 is made using the value of this limit.

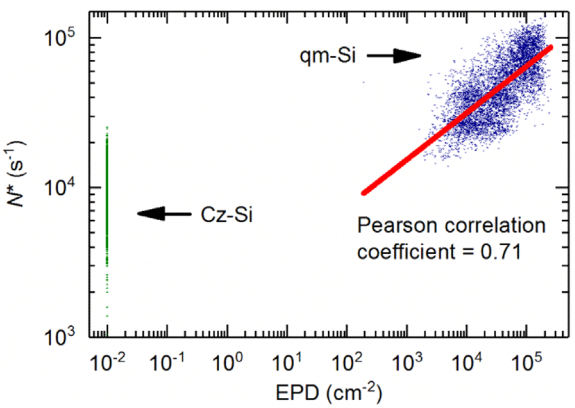

Figure 7 Normalized defect concentration, N^*, of intentionally Cu contaminated Cz-Si and mid-ingot qm-Si samples ([Cu] = $2.5 \times 10^{14}\,cm^{3}$), calculated from μPCD lifetime, as a function of EPD. The qm-Si data were fitted with a power function showing positive correlation.

In Fig. 7, an upward trend in the recombination activity of Cu-LID in qm-Si can be observed with increasing EPD. The data was fitted with a power function, and shows a clearly positive correlation. On the other hand, the recombination activity of Cu-LID in Cz-Si, which is practically dislocation-free, is considerably lower despite equal [Cu]. As considerable evidence exists that Cu-LID is a precipitation process [28], it is possible that dislocations act as heterogeneous nucleation sites [42]. This would result in an easier precipitation in the qm-Si material in comparison to Cz-Si, resulting in a higher density of recombination active precipitates. This finding is consistent with earlier results in which recombination activity of Cu-LID was found to correlate with the density of O precipitates and to be related to heterogeneous nucleation sites [26]. It is noteworthy that Cz-Si of this work had notably higher Cu-LID-limited final lifetime compared to electronic-grade Cz-Si in previous work [39], which may be due to lower density of O precipitates in the former.

3.4 Origin of LID in qm-PERC Being a considerable degradation mechanism even in the P-diffusion gettered lifetime samples, it is plausible that Cu-LID can be a significant LID mechanism also in the PERC solar cell case. In the following, the origin of LID in the qm-PERC is analyzed with a summary of the above-presented results.

Several consistencies between LID in the qm-PERC and LeTID were found. These include similarity of the timescale of both final stage of LID and regeneration to earlier LeTID observations. However, the fast timescale of LID in the qm-PERC during the first hours deviates from previous observations of LeTID. In addition, the laterally uneven degradation patterns of the qm-PERCs are contrary to homogeneous degradation reported for LeTID [22, 37].

One possible scenario is that both Cu-LID and LeTID are present simultaneously as separate mechanisms. This is supported by the similarity of LID timescale in the qm-PERC during the first hours to Sponge-LID, and consequently to Cu-LID identified in the P-diffusion gettered lifetime samples. The early fast degradation due to Cu-LID would be continued at a later stage by slow degradation due to LeTID. Since the underlying defect of LeTID is still unknown and Cu is known to be present with high probability, this scenario does not exclude a possibility that Cu could be a component of the LeTID defect (which was also discussed in Refs. [19] and [30]). The apparent absence of Cu-LID in the Cz-PERC is explained by the above result that dislocations present in the qm-PERC increase the recombination activity of Cu-LID. Dislocated materials are also known to exhibit weaker gettering efficiency than dislocation-free materials [43, 44], which may leave higher concentrations of Cu and other transition metals in the bulk after emitter formation. The possibility that several different defects can play a role is an important consideration in studies related to LID and its mitigation in PERC devices.

4 Conclusions Strong LID of 12–16%$_{rel}$ was observed in qm-Si PERC solar cells, which was not fully explainable by the LeTID mechanism. Based on the analysis of lifetime samples, Cu originating from a commonly used process step of brass wire sawing is credibly present despite the surface cleaning, emitter formation, and high cleanliness standards. The timescale of LID in the qm-PERC during the first hours was consistent with LID caused by Cu. On the other hand, LID in similarly manufactured Cz-PERC was typical to the BO defect. A possible contributor for the differing LID behavior was found from the higher sensitivity of the qm-Si material to impurity Cu, manifesting itself as higher recombination activity at similar impurity densities. This implies that Cu defects may cause a considerable LID in PERC solar cells, the strength of which seems to correlate with the density of extended defects.

Acknowledgements The work has been funded through the European Research Council under the European Union's FP7 Programme ERC Grant Agreement No. 307315. This work was supported by Finnish TEKES (40329/14) agencies under SolarEra.Net FP7 European Network. The authors also acknowledge Dr. Chiara Modanese for valuable comments for the manuscript.

References

[1] M. A. Green, Sol. Energy Mater. Sol. Cells **143**, 190 (2015).
[2] J. Schmidt, B. Lim, D. Walter, K. Bothe, S. Gatz, T. Dullweber, and P. P. Altermatt, IEEE J. Photovolt. **3**, 114 (2013).
[3] T. Dullweber and J. Schmidt, IEEE J. Photovolt. **6**, 1366 (2016).
[4] J. H. Wong, M. Royapoor, and C. W. Chan, Renew. Sustainable Energy Rev. **58**, 608 (2016).
[5] G. Coletti, Prog. Photovolt: Res. Appl. **21**, 1163 (2013).
[6] C. Donolato, J. Appl. Phys. **84**, 2656 (1998).
[7] H. J. Möller, C. Funke, M. Rinio, and S. Scholz, Thin Solid Films **487**, 179 (2005).
[8] E. Wang, H. Wang, and H. Yang, Int. J. Photoenergy **2016**, 1 (2016).
[9] N. Stoddard, W. Bei, I. Witting, M. Wagener, P. Yongkook, G. Rozgonyi, and R. Clark, Solid State Phenom. **131-133**, 1 (2008).
[10] T. Kaden, K. Petter, R. Bakowskie, Y. Ludwig, R. Lantzsch, D. Raschke, S. Rupp, and T. Spiess, Energy Procedia **27**, 103 (2012).
[11] X. Gu, X. Yu, K. Guo, L. Chen, D. Wang, and D. Yang, Sol. Energy Mater. Sol. Cells **101**, 95 (2012).
[12] N. Stoddard, B. Gründig-Wendrock, A. Krause, D. Oriwol, M. Bertoni, T. U. Naerland, I. Witting, and L. Sylla, J. Cryst. Growth **452**, 272 (2016).
[13] J. Schmidt, A. G. Aberle, and R. Hezel, in: Conference Record of the Twenty Sixth IEEE Photovoltaic Specialists Conference – 1997, Anaheim, California, USA, 29 September-3 October 1997, (IEEE, New York, 1997), pp. 13–18.
[14] K. Bothe, R. Sinton, and J. Schmidt, Prog. Photovolt: Res. Appl. **13**, 287 (2005).
[15] F. Kersten, P. Engelhart, H. C. Ploigt, A. Stekolnikov, T. Lindner, F. Stenzel, M. Bartzsch, A. Szpeth, K. Petter, J. Heitmann, and J. W. Müller, Sol. Energy Mater. Sol. Cells **142**, 83 (2015).
[16] K. Ramspeck, S. Zimmermann, H. Nagel, A. Metz, Y. Gassenbauer, B. Birkmann, and A. Seidl, in: Proceedings of the 27th European Photovoltaic Solar Energy Conference, Frankfurt, Germany, 24–28 September 2012, (WIP, Munich, Germany, 2012), pp. 861–865.
[17] F. Fertig, K. Krauß, and S. Rein, Phys. Status Solidi RRL **9**, 41 (2015).
[18] K. Krauss, F. Fertig, D. Menzel, and S. Rein, Energy Procedia **77**, 599 (2015).
[19] K. Nakayashiki, J. Hofstetter, A. E. Morishige, T. A. Li, D. B. Needleman, M. A. Jensen, and T. Buonassisi, IEEE J. Photovolt. **6**, 860 (2016).
[20] F. Kersten, J. Heitmann, and J. W. Müller, Energy Procedia **92**, 828 (2016).
[21] A. E. Morishige, M. A. Jensen, D. B. Needleman, K. Nakayashiki, J. Hofstetter, T. T. A. Li, and T. Buonassisi, IEEE J. Photovolt. **6**, 1466 (2016).
[22] T. Luka, S. Großer, C. Hagendorf, K. Ramspeck, and M. Turek, Sol. Energy Mater. Sol. Cells **158**, 43 (2016).
[23] C. Fahrland, Y. Ludwig, F. Kersten, and K. Petter, in: 2014 IEEE 40th Photovoltaic Specialist Conference (PVSC), Denver, Colorado, USA, 2014, (IEEE, New York, 2014), pp. 135–139.
[24] I. Tarasov and O. Ostapenko, in: Eighth Workshop on Crystalline Silicon Solar Cell Materials and Processes, Copper Mountain, Colorado, USA, 17–19 August 1998, (NREL, Golden, CO, USA, 1998), pp. 207–210.
[25] M. Yli-Koski, M. Palokangas, A. Haarahiltunen, H. Väinölä, J. Storgårds, H. Holmberg, and J. Sinkkonen, J. Phys. Condens. Matter **14**, 13119 (2002).
[26] H. Väinölä, E. Saarnilehto, M. Yli-Koski, A. Haarahiltunen, J. Sinkkonen, G. Berenyi, and T. Pavelka, Appl. Phys. Lett. **87**, 032109 (2005).
[27] J. Lindroos and H. Savin, J. Appl. Phys. **116**, 234901 (2014).
[28] A. Inglese, J. Lindroos, H. Vahlman, and H. Savin, J. Appl. Phys. **120**, 125703 (2016).
[29] T. Turmagambetov, S. Dubois, J. P. Garandet, B. Martel, N. Enjalbert, J. Veirman, and E. Pihan, Phys. Status Solidi C **11**, 1697 (2014).
[30] T. Luka, M. Turek, S. Großer, and C. Hagendorf, Phys. Status Solidi RRL **11**, 1600426 (2017).
[31] Y. Boulfrad, J. Lindroos, M. Wagner, F. Wolny, M. Yli-Koski, and H. Savin, Appl. Phys. Lett. **105**, 182108 (2014).
[32] M. W. Jenkins, J. Electrochem. Soc. **124**, 757 (1977).
[33] F. Wolny, T. Weber, M. Müller, and G. Fischer, Energy Procedia **38**, 523 (2013).
[34] A. Herguth, G. Schubert, M. Kaes, and G. Hahn, in: Conference Record of the2006 IEEE 4th World Conference on Photovoltaic Energy Conversion, WCPEC-4, Waikoloa, Hawaii, USA, 2006, (IEEE, New York, 2007), pp. 940–943.
[35] B. Lim, K. Bothe, and J. Schmidt, Phys. Status Solidi RRL **2**, 93 (2008).
[36] D. N. R. Payne, C. E. Chan, B. J. Hallam, B. Hoex, M. D. Abbott, S. R. Wenham, and D. M. Bagnall, Phys. Status Solidi RRL **10**, 237 (2016).
[37] D. Bredemeier, D. Walter, S. Herlufsen, and J. Schmidt, AIP Adv. **6**, 035119 (2016).

[38] J. Lindroos, Y. Boulfrad, M. Yli-Koski, and H. Savin, J. Appl. Phys. **115**, 154902 (2014).
[39] A. Inglese, J. Lindroos, and H. Savin, Appl. Phys. Lett. **107**, 052101 (2015).
[40] F. Buchholz, E. Wefringhaus, and G. Schubert, Energy Procedia **27**, 287 (2012).
[41] S. Meyer, S. Wahl, and C. Hagendorf, Energy Procedia **92**, 369 (2016).
[42] M. Seibt, V. Kveder, W. Schröter, and O. Voß, Phys. Status Solidi A **202**, 911 (2005).
[43] A. Bentzen, A. Holt, R. Kopecek, G. Stokkan, J. S. Christensen, and B. G. Svensson, J. Appl. Phys. **99**, 093509 (2006).
[44] S. Castellanos, K. E. Ekstrom, A. Autruffe, M. A. Jensen, A. E. Morishige, J. Hofstetter, P. Yen, B. Lai, G. Stokkan, C. Del Canizo, and T. Buonassisi, IEEE J. Photovolt. **6**, 632 (2016).